

1980

Purification, properties, and kinetics of D-ribulokinase from *Aerobacter aerogenes*

Mark M. Stayton
Iowa State University

Follow this and additional works at: <https://lib.dr.iastate.edu/rtd>

 Part of the [Biochemistry Commons](#)

Recommended Citation

Stayton, Mark M., "Purification, properties, and kinetics of D-ribulokinase from *Aerobacter aerogenes*" (1980). *Retrospective Theses and Dissertations*. 7134.
<https://lib.dr.iastate.edu/rtd/7134>

This Dissertation is brought to you for free and open access by the Iowa State University Capstones, Theses and Dissertations at Iowa State University Digital Repository. It has been accepted for inclusion in Retrospective Theses and Dissertations by an authorized administrator of Iowa State University Digital Repository. For more information, please contact digirep@iastate.edu.

INFORMATION TO USERS

This was produced from a copy of a document sent to us for microfilming. While the most advanced technological means to photograph and reproduce this document have been used, the quality is heavily dependent upon the quality of the material submitted.

The following explanation of techniques is provided to help you understand markings or notations which may appear on this reproduction.

1. The sign or "target" for pages apparently lacking from the document photographed is "Missing Page(s)". If it was possible to obtain the missing page(s) or section, they are spliced into the film along with adjacent pages. This may have necessitated cutting through an image and duplicating adjacent pages to assure you of complete continuity.
2. When an image on the film is obliterated with a round black mark it is an indication that the film inspector noticed either blurred copy because of movement during exposure, or duplicate copy. Unless we meant to delete copyrighted materials that should not have been filmed, you will find a good image of the page in the adjacent frame.
3. When a map, drawing or chart, etc., is part of the material being photographed the photographer has followed a definite method in "sectioning" the material. It is customary to begin filming at the upper left hand corner of a large sheet and to continue from left to right in equal sections with small overlaps. If necessary, sectioning is continued again—beginning below the first row and continuing on until complete.
4. For any illustrations that cannot be reproduced satisfactorily by xerography, photographic prints can be purchased at additional cost and tipped into your xerographic copy. Requests can be made to our Dissertations Customer Services Department.
5. Some pages in any document may have indistinct print. In all cases we have filmed the best available copy.

University
Microfilms
International

300 N. ZEEB ROAD, ANN ARBOR, MI 48106
18 BEDFORD ROW, LONDON WC1R 4EJ, ENGLAND

8106059

STAYTON, MARK M.

PURIFICATION, PROPERTIES, AND KINETICS OF D-RIBULOKINASE
FROM AEROBACTER AEROGENES

Iowa State University

PH.D.

1980

University
Microfilms
International 300 N. Zeeb Road, Ann Arbor, MI 48106

Purification, properties, and kinetics
of D-ribulokinase from Aerobacter aerogenes

by

Mark M. Stayton

A Dissertation Submitted to the
Graduate Faculty in Partial Fulfillment of the
Requirements for the Degree of
DOCTOR OF PHILOSOPHY

Department: Biochemistry and Biophysics
Major: Biochemistry

Approved:

Signature was redacted for privacy.

In Charge of Major Work

Signature was redacted for privacy.

For the Major Department

Signature was redacted for privacy.

For the Graduate College

Iowa State University
Ames, Iowa

1980

TABLE OF CONTENTS

	Page
ABBREVIATIONS	vi
INTRODUCTION	1
EXPERIMENTAL PROCEDURE	7
RESULTS	22
DISCUSSION	49
LITERATURE CITED	55
APPENDIX	58
ACKNOWLEDGMENTS	61

LIST OF FIGURES

	Page
Figure 1. Aldopentose and pentitol metabolism by <u>Aerobacter aerogenes</u>	3
Figure 2. S200 gel chromatography of D-ribulokinase	13
Figure 3. A plot of elution volume (from an S200 gel column) <u>versus</u> the log of the molecular weight for various standard proteins	16
Figure 4. A plot of electrophoretic mobility (on SDS polyacrylamide gels) <u>versus</u> the log of the subunit molecular weight for various standard proteins	18
Figure 5. A photograph of an analytical disc gel of purified D-ribulokinase	24
Figure 6. Plot of the reciprocal of initial velocity (v) <u>versus</u> the reciprocal of the molar concentration of D-ribulose at various, fixed concentrations of MgATP ²⁻	27
Figure 7. Plot of the reciprocal of initial velocity (v) <u>versus</u> the reciprocal of the molar concentration of MgATP ²⁻ at various, fixed concentrations of D-ribulose	29
Figure 8. Plot of the reciprocal of initial velocity (v) <u>versus</u> the reciprocal of the molar concentration of MgATP ²⁻ at various, fixed concentrations of AMP ²⁻	33
Figure 9. Plot of the reciprocal of initial velocity (v) <u>versus</u> the reciprocal of the molar concentration of D-ribulose at various fixed concentrations of AMP ²⁻	35
Figure 10. Plot of the reciprocal of initial velocity (v) <u>versus</u> the reciprocal of the molar concentration of D-ribulose at various fixed concentrations of dihydroxyacetone	37

- Figure 11. Plot of the reciprocal of initial velocity (v) versus the reciprocal of the molar concentration of MgATP^{2-} at various, fixed concentrations of dihydroxyacetone 41
- Figure 12. Plot of the reciprocal of initial velocity (v) versus the reciprocal of the molar concentration of MgATP^{2-} at various, fixed concentrations of MgADP^{1-} 46
- Figure 13. Plot of the reciprocal of initial velocity (v) versus the reciprocal of the molar concentration of D-ribulose at various, fixed concentrations of MgADP^{1-} 48
- Figure 14. A theoretical plot of initial velocity (v) versus the molar concentration of D-ribulose 53

LIST OF TABLES

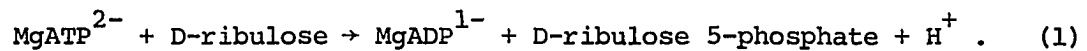
	Page
Table I. Summary of the purification of D-ribulokinase from <u>A. aerogenes</u>	23
Table II. D-ribulokinase kinetic constants	30
Table III. Isotope partitioning with [³ H]D-ribulose	43

ABBREVIATIONS

ADP	Adenosine-5'-diphosphate
AMP	Adenosine-5'-monophosphate
ATP	Adenosine-5'-triphosphate
DEAE	Diethylaminoethyl
EDTA	Ethylenediamine tetraacetate
HEPES	4-(2-hydroxyethyl)-1-piperazine-ethanesulfonic acid
M_r	Relative molecular mass
NAD	Nicotinamide adenine dinucleotide
NADH	Reduced NAD
SDS	Sodium dodecyl sulfate
V_e	Elution volume

INTRODUCTION

The utilization of ribitol in Aerobacter aerogenes involves the action of two adaptive enzymes, ribitol dehydrogenase (EC 1.1.1.56) and D-ribulokinase (EC 2.7.1.47) before its entry into the oxidative pentose cycle. Since the discovery of ribitol dehydrogenase in 1958 by Wood and Tai (1) and Fromm (2), a series of studies have reported its purification (3,4), crystallization (5), and initial-rate kinetics (3,6). D-ribulokinase, however, has not been studied extensively, partly because of its instability and the lack of a suitable purification scheme. The enzyme catalyzes the following reaction:



The partial purification, reaction stoichiometry, pH optimum, and apparent Michaelis constants have been reported for D-ribulokinase (7).

Its role in bacterial metabolism has been extensively examined (8,9,10,11). Aerobacter aerogenes is unusual among bacteria in that it can utilize as its sole carbon source at least seven of the eight aldopentoses (D- and L-arabinose, D- and L-xylose, D- and L-lyxose, D-ribose and possibly L-ribose) and all four pentitols (ribitol, D- and L-arabitol and xylitol) (11). This is quite remarkable because only three of the aldopentoses (D-ribose, L-arabinose and D-xylose) and only two of the pentitols (ribitol and D-arabitol) are considered to be available as growth substrates in nature (12). Growth rates on these compounds vary widely. Growth occurred within 24 h (at 26°C) on media

containing D-xylose, L-arabinose, D-ribose, D-arabitol or ribitol. Growth was complete within 2 days on D-arabinose or L-arabitol, within 4 days on D-lyxose or xylitol and within 3 to 4 weeks on L-xylose (11).

Fermentation studies with specifically labelled pentoses demonstrated that these compounds share a common catabolic pathway. For example, consider the fermentation of L-arabinose and D-arabinose, which are each labelled with ^{14}C at the one position. No significant differences were found in the intramolecular distribution of ^{14}C in any of the fermentation products obtained from the two sugars. The lactate isolated from anaerobic cultures contained the label in both the methyl and carboxyl positions. This labelling pattern could be explained qualitatively and quantitatively assuming both sugars are metabolized via the same intermediate, a heptulose. This conclusion was strengthened and extended by studies utilizing labelled D-ribose, and D-xylose (13, 14).

The strategy for pentose utilization involves isomerization of an aldopentose to (one of the four) ketopentoses, phosphorylation of the ketopentoses and epimerization of ketopentose-5-phosphates to D-xylulose-5-phosphate, the substrate of transketolase. The exception is D-ribose, which is phosphorylated before the isomerization step. Pentitols are utilized by dehydrogenation to the ketopentose, but the remaining steps are identical. These pathways are summarized in Fig. 1 (11). Many of the individual reactions involved in the catabolism of these compounds have been examined: L-arabinose (15), L-xylose and L-lyxose (16), ribitol (2,4), D-arabitol (4,17) and L-arabitol and

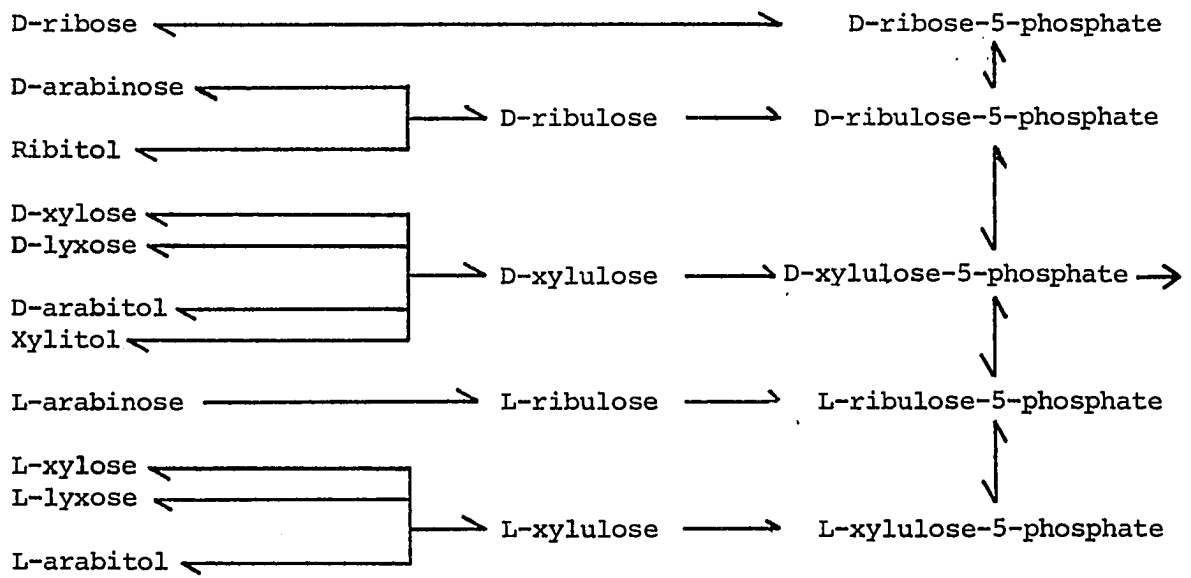


Figure 1. Aldopentose and pentitol metabolism by Aerobacter aerogenes

xylitol (18).

The carbohydrate carbon source is not necessarily the inducing agent for the enzymes of its catabolism. The coordinately controlled enzymes of ribitol catabolism, ribitol dehydrogenase and D-ribulokinase, are an example. A mutant bacterial strain of A. aerogenes was isolated, which lacked the dehydrogenase activity. This strain was unable to induce the kinase in the presence of ribitol. The analogous experiment using a kinase-negative mutant resulted in the normal induction of ribitol dehydrogenase. It was also found that A. aerogenes cells containing the inducible enzyme, L-fucose isomerase, are capable of isomerizing D-arabinose to D-ribulose. The isomerization of D-arabinose to D-ribulose in dehydrogenase-negative cells resulted in the induction of D-ribulokinase (8). These data establish that D-ribulose rather than ribitol acts as the inducer of the two enzymes.

Constitutive mutants for ribitol dehydrogenase and D-ribulokinase can be isolated by growth on xylitol (11, 18). This is possible because ribitol dehydrogenase catalyzes the first step in xylitol metabolism and yet xylitol does not induce the enzyme. Only those cells constitutive for ribitol dehydrogenase will survive on xylitol. In this instance, enzyme overproduction generally occurs via gene doubling (12,19). In Klebsiella aerogenes W-70, by contrast, mutations which permit constitutive synthesis of both enzymes have been mapped at locations postulated to represent the regulatory genes of the ribitol catabolic pathway (20). The use of the alternate substrate, xylitol, has been

developed into a model system to study the molecular evolution of enzymes (12,19,21,22,23,24).

E. coli strains can also be isolated that are constitutive for ribitol dehydrogenase and D-ribulokinase. Such strains concomitantly acquire toxicity to polyols such as galactitol and L-arabitol. Strains selected for resistance to these polyols have D-ribulokinase structural gene mutations (25). The conclusion was that D-ribulokinase phosphorylates these compounds to toxic substances.

It has been observed that D-ribulokinase activity in A. aerogenes can be induced by growth on several compounds other than ribitol. These compounds include D-arabinose, xylitol, D-ribose L-xylulose and L-arabinose (11). It is possible that all inductions of D-ribulokinase activity are not due to production of the same protein. To resolve this question, an examination of the physical and immunological properties of the pentitol dehydrogenases and pentulokinases was undertaken (26). Seven enzymatic activities were studied. The xylitol dehydrogenase activity and ribitol dehydrogenase activity were found to result from the same protein. Each of the remaining reactions (including the phosphorylation of D-ribulose) was shown to be catalyzed by a single, unique enzyme.

Mortlock et al. (26) described a generalized scheme for the purification of the pentulokinases. It involved protamine sulfate and ammonium sulfate fractionations, a heat treatment, DEAE cellulose chromatography and Alumina C gel treatment. A 216-fold purification of

D-ribulokinase was achieved, although the purity of the final product was low when compared with the specific activity achieved by Stayton and Fromm (27). The enzyme was very unstable, losing most of its activity in two weeks. A sedimentation coefficient, S_{20} , of about 6.2 was empirically obtained from sucrose gradient centrifugation. If it is assumed that the protein is spherical with a partial specific volume of $0.73 \text{ cm}^3 \text{ g}^{-1}$ [as Mortlock et al. (26) did for the D-arabitol and ribitol dehydrogenases] a molecular weight of 110,000 can be calculated for D-ribulokinase.

The present report describes a protocol for purifying and stabilizing D-ribulokinase. Estimates of the molecular weight and the subunit molecular weight were obtained, which suggest that the enzyme exists as a dimer of identical subunits. In addition, kinetic studies present evidence supporting a steady-state random Bi Bi kinetic mechanism for D-ribulokinase.

EXPERIMENTAL PROCEDURE

Materials

ATP, NADH, D-ribose and protamine sulfate were products of Sigma. D-ribose was recrystallized twice from absolute ethanol. HEPES,¹ Ultrol brand, was obtained from Calbiochem. Enzyme-grade ammonium sulfate was purchased from Schwartz Mann. Pyruvate kinase and lactate dehydrogenase were obtained from Boehringer-Mannheim. [¹⁴C]ATP (51.1 mCi/mmol) was purchased from ICN, and [³H]sodium borohydride (3 Ci/mmol) was obtained from Amersham-Searle. D-ribulose was synthesized from D-arabinose by base-catalyzed epimerization according to the procedure of Glatthaar and Reichstein (28) and isolated as the o-nitrophenylhydrazone derivative. The same derivative of L-ribulose was a gift from Dr. W. A. Wood, Michigan State University. Decomposition of the hydrazone derivatives, to yield the free monosaccharide, was accomplished with benzaldehyde by using the procedure of Reichstein (29). D-ribulose-5-phosphate was synthesized and isolated according to the procedure of Fromm (7). Microgranular, pre-swollen, DEAE cellulose (DE 52) and DEAE paper (DE 81) were both products of Whatman. Blue dextran and Sephacryl S-200 Superfine were obtained from Pharmacia. All reagents for polyacrylamide gel electrophoresis were supplied by Bio-Rad Laboratories. Low-ion water was obtained by passing distilled water through a Barnstead High Capacity ion exchange column and a Continental water deionizer

¹Abbreviations used: Hepes, N-2-hydroxyethylpiperazine-N'-2-ethane sulfonic acid.

(Continental Deionized Water Service, North Kansas City, MO). All other reagents were of the highest possible purity.

Bacteria

A. aerogenes (ATCC 9621), from a lyophilized culture and maintained on refrigerated agar slants containing minimal salts and ribitol as the sole carbon source, was the parent bacterial strain. A mutant strain, constitutive for both ribitol dehydrogenase and D-ribulokinase, was isolated by selective growth on a medium containing minimal salts and 0.5% xylitol (30). The constitutive strain was grown on a sterile 500-ml inorganic salt medium (31) supplemented with 0.5% ribitol. This starter culture was divided equally and used to inoculate 10, 2-liter flasks containing 400 ml of the inorganic salt medium supplemented with 0.5% glucose and 0.5% yeast extract. The cells were grown at 37° with vigorous shaking, harvested, and washed, and extracts were prepared by using a French pressure cell (32). The extracts were not allowed to stand overnight, but were used immediately.

Enzyme Assays

Standard assay conditions were 150 mM Hepes (pH 7.7), 5.0 mM D-ribulose, 5.0 mM ATP, 6.0 mM MgCl₂, and 15.0 mM 2-mercaptoethanol. A unit of D-ribulokinase activity was defined as the amount of enzyme that catalyzed the phosphorylation of 1 μmol of D-ribulose per minute at 37° under standard assay conditions.

The following stopped time procedure was used during the purification of D-ribulokinase. The usual ADP-coupled assay (26) was not used

because of prohibitively high levels of ribitol dehydrogenase, ATPase, and NADH oxidase during the early stages of the purification. Assays (0.75 ml) were preincubated at 37^o in a controlled-temperature bath. The reactions were started by the addition of enzyme and terminated by boiling for 1.0 min. After cooling on ice, a 0.50-ml aliquot was analyzed for ADP by measuring NADH oxidation in the presence of phosphoenolpyruvate, pyruvate kinase, and lactate dehydrogenase. Controls were done in which the enzyme was boiled before being incubated with the reaction mixture. The linearity of product versus time progress curves was established by removing aliquots of the reaction mixtures at different time periods after enzyme addition. Protein was determined with a Coomassie blue protein assay obtained from Bio-Rad.

D-Ribulokinase Purification

This scheme involves extensive modifications of earlier procedures (26). All steps in the purification were carried out at 4^o.

Protamine sulfate treatment

The cell-free extract of A. aerogenes was diluted to a protein concentration of 10 mg/ml with 5 mM potassium phosphate (pH 7.5), 1 mM EDTA. Solid ammonium sulfate was added to 0.1 M, followed by dropwise addition of 0.1 volume of a 40 mg/ml protamine sulfate solution. The mixture was stirred for 10 min and then centrifuged at 16,000 x g for 10 min, the precipitate was dissolved in a buffer containing 100 mM potassium phosphate (pH 7.5), 5 mM 2-mercaptoethanol, and 1 mM EDTA.

This protein solution was dialyzed overnight on a rocking dialyzer against 2.0 liters of the same buffer. For the remainder of the purification, all buffers contain 5 mM 2-mercaptoethanol, 1 mM EDTA, and the stated concentration of potassium phosphate at pH 7.5.

DEAE cellulose chromatography

DEAE cellulose, equilibrated in 100 mM buffer, was added with stirring to the dialyzed protein solution until no D-ribulokinase activity could be detected in the supernatant fluid. A 5 cm x 11 cm column was then prepared and washed with 100 mM buffer until the absorbance of the wash at 280 nm had leveled off at about 0.05. A linear gradient (2.0 liters) from 100 to 250 mM buffer was applied, and 10-ml fractions were collected. The D-ribulokinase activity eluted as a trailing shoulder on a large inactive protein peak.

Gel filtration

The combined fractions were concentrated to 20 ml by ultrafiltration and were applied to a 2.5 x 92 cm Sephacryl S-200 column that had been with equilibrated 100 mM buffer. The flow rate was maintained at 0.5 ml per min with a peristaltic pump, and 2.5-ml fractions were collected.

Second DEAE cellulose chromatography

The combined fractions from the previous gel column were applied directly to a 1.5 x 11.5 cm DEAE cellulose column equilibrated with 100 mM buffer. The column was washed with one column volume of 100 mM buffer, followed by three column volumes of 150 mM buffer. The enzyme

was then eluted with a linear gradient (1.0 liters) from 150 to 250 mM buffer, taking 10-ml fractions.

Final gel filtration

The active fractions from the second anion exchange column were combined and concentrated by ultrafiltration to about 3 ml. This sample was applied to the 2.5 x 92 cm Sephacryl S-200 column as before. The enzyme activity eluted coincident with a symmetrical protein peak and was well-separated from a small, inactive, higher-molecular-weight peak (Fig. 2).

Gel Electrophoresis

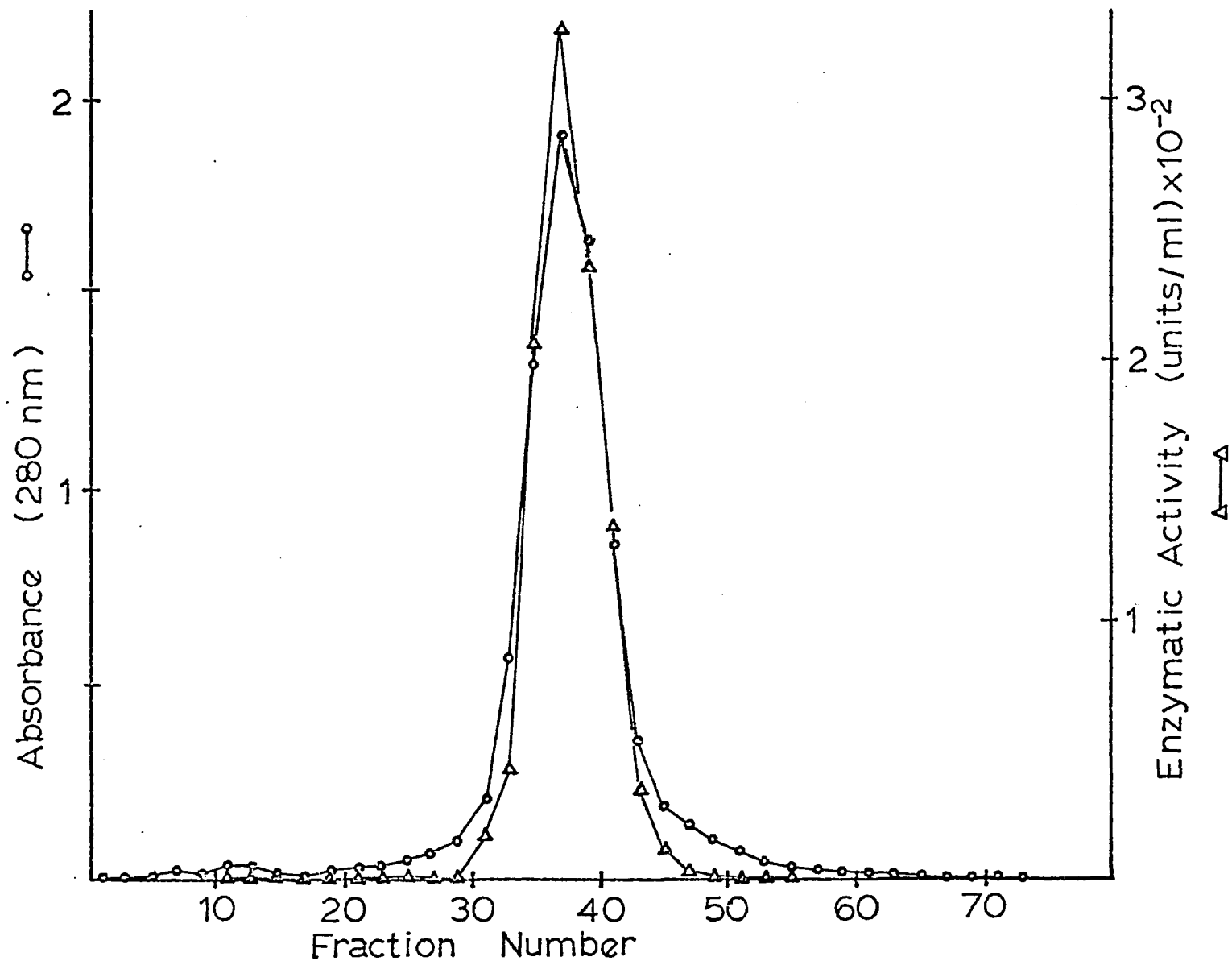
Native gels were prepared by using the procedure of Davis (33). Protein was stained with Coomassie brilliant blue R-250. The active band was identified by running two identical gels in parallel, staining one for protein and excising the appropriate portions of the other gel. These gel sections were crushed in 0.75 ml of the standard assay mixture, incubated at 37°C for 10 min, stopped by boiling, and analyzed for ADP. Sodium dodecylsulfate gel electrophoresis was carried out by using the system of Weber and Osborn (34) with gels made 7% in acrylamide.

Molecular Weight Determinations

The molecular weight of native D-ribulokinase was determined by gel filtration on a Sephacryl S-200 column with various standard proteins of known molecular weight as described by Andrews (35). The column (2.5 x 91 cm) was equilibrated with a buffer containing 100 mM potassium

Figure 2. S200 gel chromatography of D-ribulokinase

The enzymatically active fractions from the second DEAE cellulose column were combined, concentrated and applied to a 2.5 x 92 cm Sephacryl S200 column. The column was eluted with 100 mM potassium phosphate buffer (pH 7.5) containing 5 mM 2-mercaptoethanol and 1 mM EDTA. The fraction size was 2.5 ml and the first 130 ml were collected and discarded before fractions were taken. Fractions 34 through 41 were combined.



phosphate (pH 7.5), 5 mM 2-mercaptoethanol, and 1 mM EDTA. The temperature was maintained at 5^o, the flow rate was established at 30.0 ml per hour with a peristaltic pump, and 2.0-ml fractions were collected. Blue dextran was read at 620 nm, ovalbumin at 280 nm, and cytochrome c at 415 nm. Alcohol dehydrogenase activity was measured by following the reduction of NAD by ethanol. Lactate dehydrogenase was assayed by following NADH oxidation in the presence of PEP, ADP, and lactate dehydrogenase. The standard curve is given in Fig. 3.

The subunit molecular weight was estimated by using the procedure of Weber and Osborn (34) with the following standards, ovalbumin, glyceraldehyde phosphate dehydrogenase, pyruvate kinase, and serum albumin (Fig. 4).

Synthesis of [³H] D-Ribulose

The synthesis was accomplished in two steps; reduction of D-ribose to [³H] ribitol with [³H] NaBH₄, followed by oxidation, catalyzed by ribitol dehydrogenase, of the [³H] ribitol to [³H] D-ribulose. One-tenth ml of 70 mM D-ribose and 10 μ l of 0.1 M [³H] NaBH₄ (3 Ci/mmol) were combined and kept at room temperature for 10 h. To remove the borate, 0.5 ml of methanol was added, and the mixture was lyophilized. This lyophilization from methanol was repeated twice. To the mixture was added 0.6 ml of a reaction mixture containing 42 mM potassium phosphate buffer (pH 7.5), 267 mM potassium pyruvate, 0.83 mM NAD, 20 mM ribitol, and 1 unit each of ribitol dehydrogenase and lactate dehydrogenase. This mixture was kept overnight at room temperature and

Figure 3. A plot of elution volume (from an S200 gel column) versus the log of the molecular weight for various standard proteins

The standard proteins, listed according to increasing molecular weight, were cytochrome C, ovalbumin, alcohol dehydrogenase, lactate dehydrogenase and pyruvate kinase. The pointer indicates the position of D-ribulokinase on the standard curve. A molecular weight of 116,000 was calculated. Other experimental details are described under Experimental Procedure.

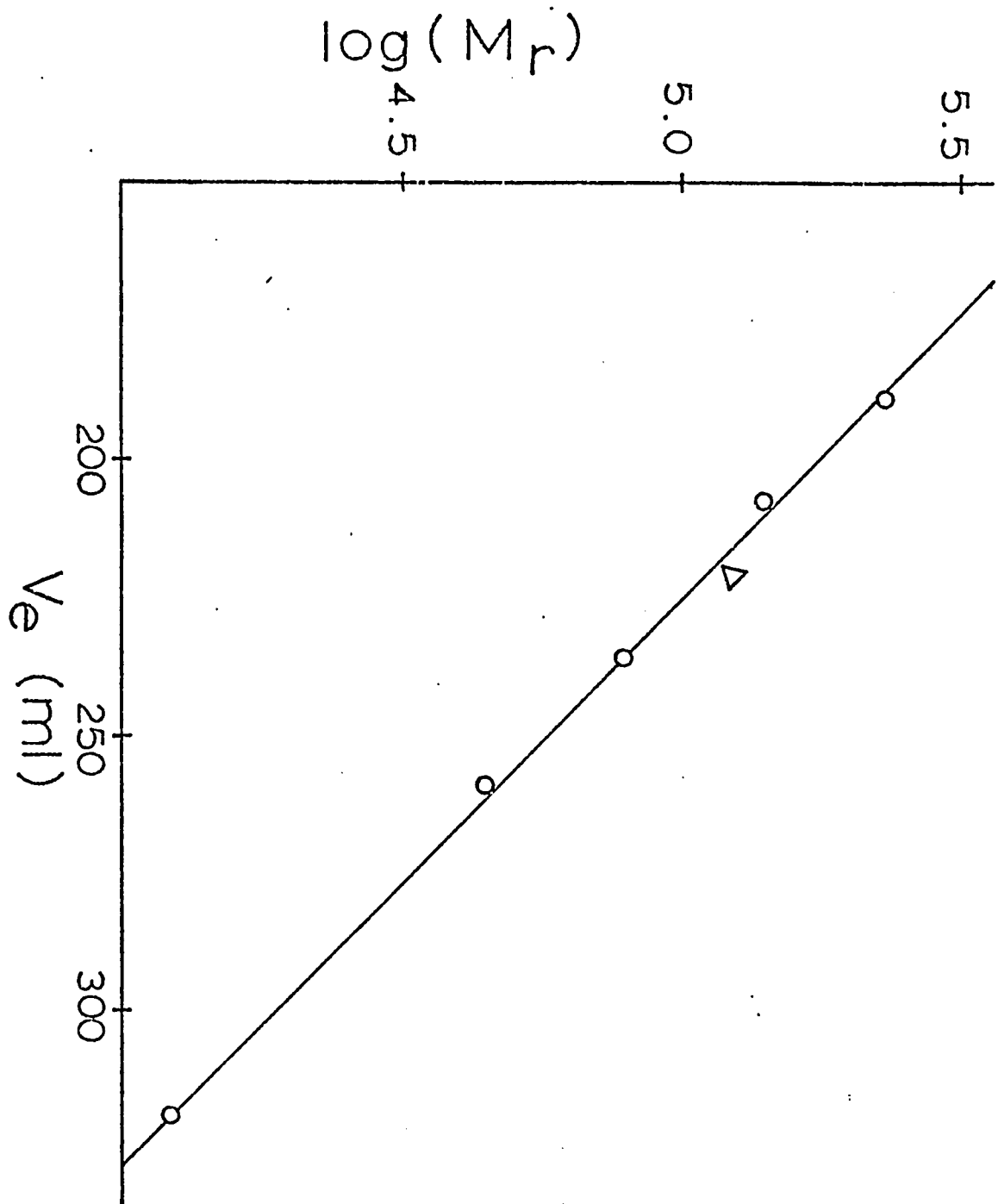
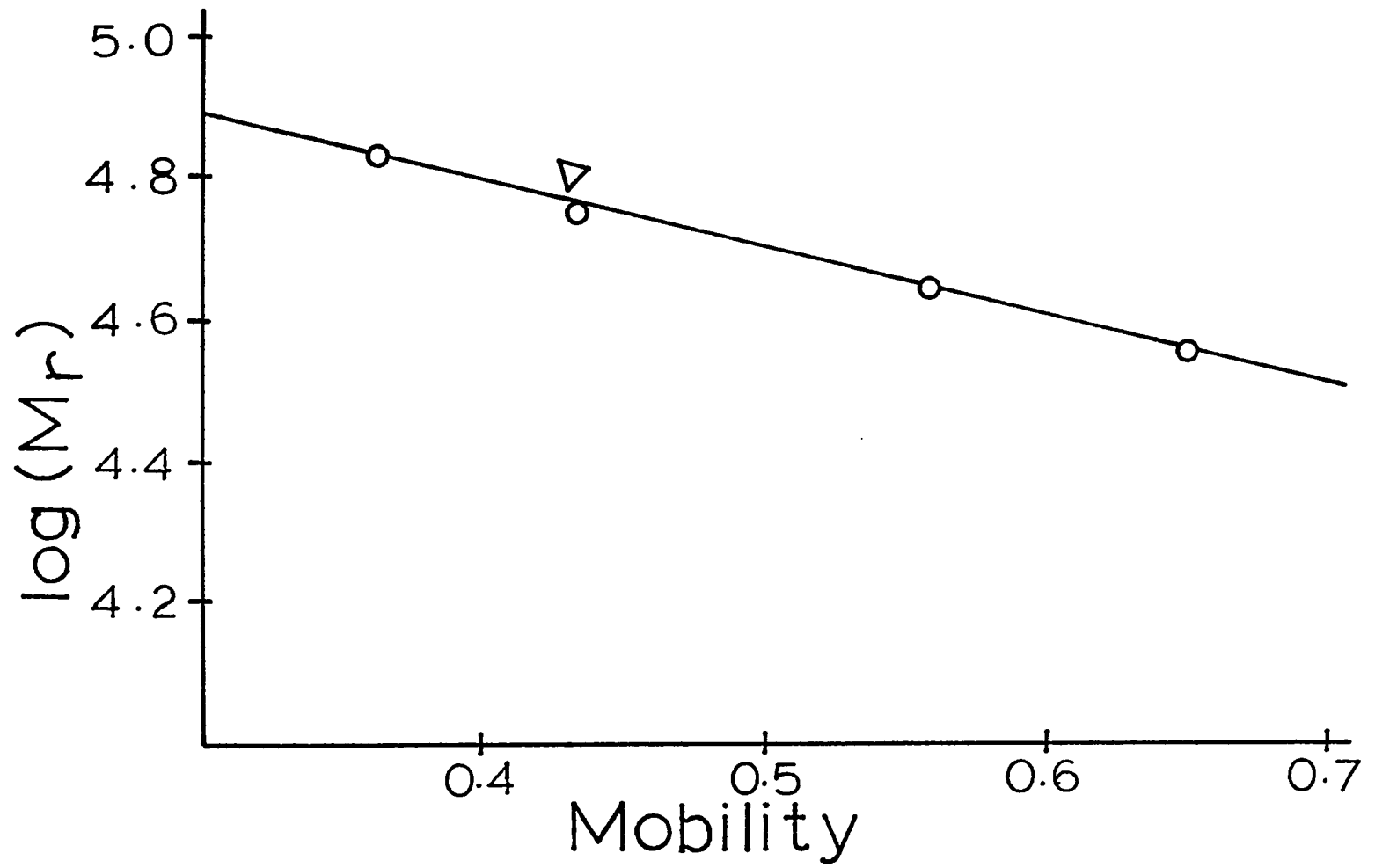


Figure 4. A plot of electrophoretic mobility (on SDS polyacrylamide gels) versus the log of the subunit molecular weight for various standard proteins

The standard proteins, listed according to increasing subunit molecular weight, were glyceraldehyde 3-phosphate dehydrogenase, ovalbumin, pyruvate kinase, and serum albumin. The pointer indicates the position of D-ribulokinase on the standard curve. A subunit molecular weight of 59,000 was calculated. Other experimental details are described under Experimental Procedure.



was then washed onto a 1.1 x 3.1 cm AG1-X2 (Cl^-) column. The column was washed with four, 3.0-ml aliquots of deionized water. The pass-through volume and all four washes were combined, frozen, and lyophilized. The yield was 4.3 μmoles of [^3H] D-ribulose with a specific activity of 4.27×10^{12} cpm/mole.

Kinetic Studies

The kinetics were carried out at 28° by following the formation of [^{14}C] ADP from [^{14}C] ATP. The 0.3-ml reaction mixtures contained 20 mM Hepes (pH 7.7), 15 mM 2-mercaptoethanol, various levels of ATP, D-ribulose, and inhibitors, and a MgCl_2 concentration adjusted to give 2.0 mM free Mg^{2+} (36). Each reaction was initiated by the addition of D-ribulokinase (10 μl , 0.018 μg), incubated for 5.0 min, and stopped by the addition of 25 μl of 200 mM EDTA. Control experiments established both the linearity of the product versus time curve over the 5-min time interval at both high and low substrate levels and the efficiency of the EDTA stop. A 40- μl sample from each reaction mixture was spotted (in 10- μl aliquots) on DEAE paper along with 0.1 μmoles of carrier ADP. The chromatograms were developed according to Morrison (37). The nucleotide spots were visualized under ultraviolet light, cut out and counted in 15 ml of a toluene-based counting solution (38). Controls, in which the EDTA stop was added before the enzyme solution, were made for each concentration of ATP.

Isotope Partitioning

The protocol was adapted from that used by previous workers (39,40). Before use, the enzyme preparation was passed through a P-2 gel column (Bio-Rad) equilibrated in 20 mM Hepes (pH 7.7) and 15 mM 2-mercaptoethanol to ensure the complete removal of D-ribulose. Incubation mixtures contained 0.855 mM [^3H] D-ribulose (4.27×10^{12} cpm per mole), 20 mM Hepes (pH 7.7), 15 mM 2-mercaptoethanol, and 60 μM D-ribulokinase binding sites for D-ribulose (assuming that the enzyme is a dimer with identical subunits). After 5 min at 28 $^{\circ}$, 0.1 ml of the incubation mixture was rapidly added to a 2.0-ml solution containing 20 mM Hepes (pH 7.7), 1.0 mM ATP, 193.3 mM D-ribulose, 4.0 mM MgCl_2 , and 15 mM 2-mercaptoethanol. After 2 s of vigorous agitation using a vortex mixer, 0.1 ml of 556 mM EDTA was added to stop the reaction, and the mixture was immediately placed on ice. Each reaction mixture was added to a 2-ml AG1-X2 (Cl^-) column, and the column was washed with 100 ml of deionized water. The [^3H] D-ribulose-5-P was eluted with three 4.0-ml aliquots of a 0.1 N HCl, 0.1 M KCl solution. The aliquots were combined, and 5.0 ml was counted in 15 ml of Bray's solution (41).

Statistical Analysis

Statistical analysis of the kinetic data was done with the Omnitab computer program of Siano et al. (42) using an α value of zero. Each experiment was fitted to three models, noncompetitive, competitive, and uncompetitive types of inhibition. The best-fit model was selected on the basis of the appropriate F-test. The experimental points and the

best-fit lines were plotted with the use of SIMPLOTTER, a high-level computer plotting system provided by the Iowa State University Computation Center.

RESULTS

Purification of D-Ribulokinase

In 1965, Mortlock et al. (26) reported a generalized scheme for the partial purification of a group of inducible kinases, including D-ribulokinase, and dehydrogenases from A. aerogenes. These authors reported that the kinase was unstable, losing a significant amount of activity in 2 weeks. To allow mechanistic studies, we modified the procedure extensively, achieving a stable, pure D-ribulokinase preparation. The use of an A. aerogenes mutant constitutive for D-ribulokinase (and ribitol dehydrogenase) was important in the purification because this mutant yielded approximately 10-fold more D-ribulokinase per gram of cells than did the parent strain.

A summary of a typical preparation is given in Table I. The yield of enzyme was improved by working rapidly and washing the initial DEAE cellulose column free of inactive protein by the end of the first day. During the purification, the enzyme was stabilized by adding 5 mM 2-mercaptoethanol and 1 mM EDTA to the buffers and by including 0.5 mM D-ribulose in the final enzyme preparation. An activity loss of about 10 percent was observed over a 6-month period.

The enzyme migrated as a single protein band during sodium dodecyl sulfate gel electrophoresis and during S-200 gel filtration (Fig. 2); however, two minor contaminants were evident after discontinuous gel electrophoresis (Fig. 5). D-ribulokinase was identified as the major band as described in the experimental procedure. Upon the basis of

Table I. Summary of the purification of D-ribulokinase from A. aerogenes

Step	Volume (ml)	Protein (mg)	Activity (units)	Specific Activity (units/mg)	Purifi- cation	Yield
Cell-free extract	700	5,810	19,250	3.3	1	100
Protamine sulfate treatment	737	4,179	17,170	4.1	1.2	89
Ammonium sulfate fractionation followed by dialysis	220	2,046	12,940	6.3	1.9	67
DEAE cellulose	990	161	6,220	38.6	11.7	32
S200 gel chromatography	60	73.2	5,160	70.5	21.4	27
Second DEAE cellulose chromatography	225	36	4,390	122	36.9	23
Final S200 gel chromatography	20.8	18.7	2,840	151.5	46	15



Figure 5. A photograph of an analytical disc gel of purified D-ribulokinase

This gel was stained for protein. The enzymatic activity of the major band was established as described in Experimental Procedure.

this evidence, the final D-ribulokinase preparation was estimated to be at least 95 percent pure.

Molecular Weight Determinations

Chromatography on a Sephacryl S-200 column was carried out in an attempt to determine the molecular weight of D-ribulokinase (Fig. 3). The value obtained, 116,000, agrees well with the value of 110,000 obtained by Mortlock *et al.* (26) from sucrose density-gradient centrifugation. The subunit molecular weight was determined by sodium dodecyl sulfate gel electrophoresis, which yielded a value of 59,000 (Fig. 4), suggesting that D-ribulokinase exists as a dimer of identical subunits. For details, see experimental procedure.

Initial-Rate Kinetics

Initial-rate kinetics were undertaken to provide some insight into the kinetic mechanism of D-ribulokinase. It is clear from Figs. 6 and 7 that both initial-rate plots are convergent and, thus, that the kinetic mechanism is sequential.² The plots are consistent with the rate expression for a general sequential mechanism (44) given in equation 2, and the computer-fitted constants and their standard deviations are listed in Table II.

$$\frac{1}{v} = \frac{1}{V_1} \left[1 + \frac{K_a}{A} + \frac{K_b}{B} + \frac{K_{ia}K_b}{A B} \right] \quad (2)$$

²The nomenclature is that of Cleland (43).

Figure 6. Plot of the reciprocal of initial velocity (v) versus the reciprocal of the molar concentration of D-ribulose at various, fixed concentrations of MgATP^{2-}

D-ribulose was varied in the range $42.7 \mu\text{M}$ to 0.384 mM . MgATP^{2-} was held at 0.545 mM (\circ), 0.182 mM (Δ), 0.109 mM , ($+$), $77.8 \mu\text{M}$ (\times), and $60.5 \mu\text{M}$ (\diamond). Other experimental details are described under Experimental Procedure.

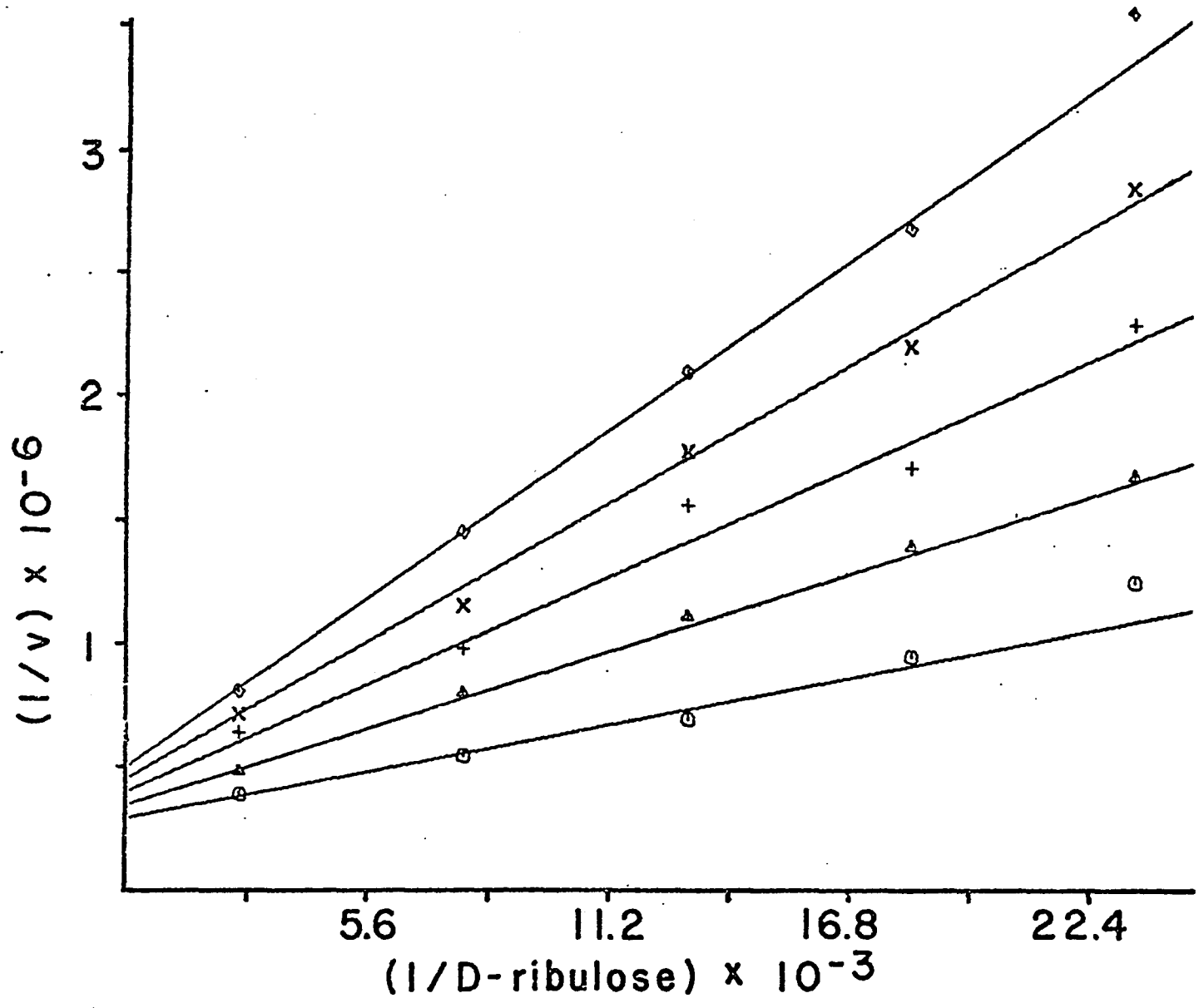


Figure 7. Plot of the reciprocal of initial velocity (v) versus the reciprocal of the molar concentration of MgATP^{2-} at various, fixed concentrations of D-ribulose

MgATP^{2-} was varied in the range $60.5 \mu\text{M}$ to 0.545 mM . D-ribulose was held at 0.384 mM (\circ), 0.128 mM (Δ), $76.8 \mu\text{M}$ ($+$), $54.9 \mu\text{M}$ (\times), and $42.7 \mu\text{M}$ (\diamond). Other experimental details are described under Experimental Procedure.

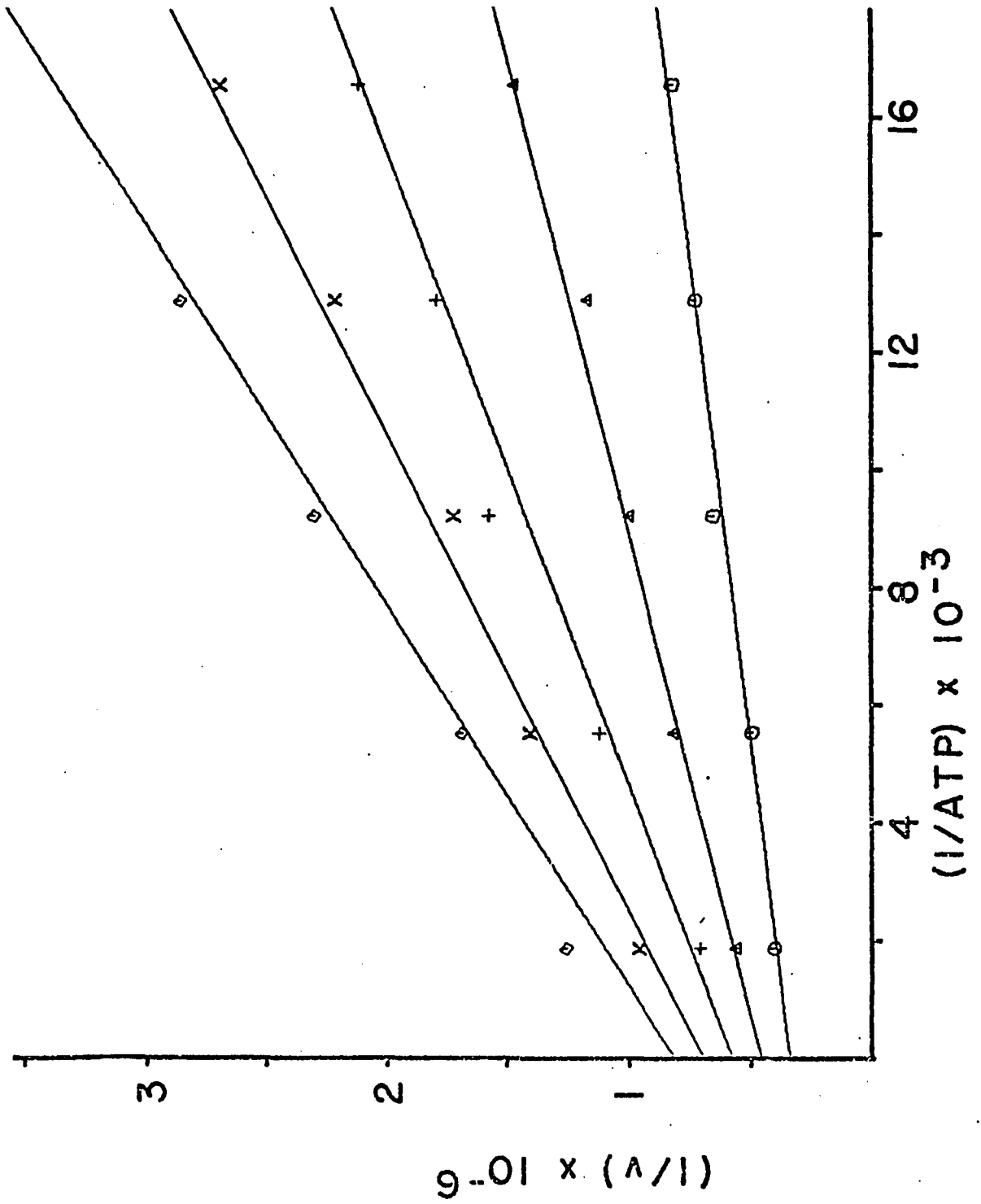


Table II. D-ribulokinase kinetic constants^a

Equilibria	Dissociation constant \pm standard deviation	
	Initial Rates (Equation 2)	
EAB = EB + A	K_a ,	$5.35 \times 10^{-5} \text{ M} \pm 9.0 \times 10^{-6}$
EAB = EA + B	K_b ,	$8.34 \times 10^{-5} \pm 9.6 \times 10^{-6}$
EA = E + A	K_{ia} ,	$2.61 \times 10^{-4} \pm 3.6 \times 10^{-5}$
EB = E + B	K_{ib} ,	$4.06 \times 10^{-4} \pm 7.9 \times 10^{-5}$
	$(V_1, 3.61 \times 10^{-6} \text{ M min}^{-1})$	
	AMP ²⁻ Inhibition (Equation 3)	
EI = E + I	K_i ,	$9.19 \times 10^{-3} \text{ M} \pm 1.9 \times 10^{-3}$
EBI = EB + I	K_{ii} ,	$8.29 \times 10^{-4} \pm 1.2 \times 10^{-4}$
EBI = EI + B	K_{iii}^b ,	$3.66 \times 10^{-5} \pm 2.0 \times 10^{-5}$
	Dihydroxyacetone Inhibition (Equation 4)	
EI = E + I	K_i ,	$1.63 \times 10^{-1} \text{ M} \pm 2.1 \times 10^{-2}$
EAI = EA + I	K_{ii} ,	$8.89 \times 10^{-2} \pm 9.6 \times 10^{-3}$
EAI = EI + A	K_{iii}^c ,	$1.42 \times 10^{-4} \pm 5.3 \times 10^{-5}$
	MgADP ¹⁻ Inhibition (Equation 6)	
EQ = E + Q	K_{iq} ,	$2.32 \times 10^{-4} \text{ M} \pm 9.7 \times 10^{-5}$
EBQ = EB + Q	K_{iq} ,	$1.98 \times 10^{-5} \pm 3.0 \times 10^{-6}$
EBQ = EQ + B	K_{ib} ,	$3.47 \times 10^{-5} \pm 1.7 \times 10^{-5}$

^aThe calculations are based on a rapid-equilibrium random Bi Bi mechanism with the formation of the E·D-ribulose·MgADP abortive.

$$^b K_{iii} = K_{ib} K_{ii} / K_i$$

$$^c K_{iii} = K_{ia} K_{ii} / K_i$$

The following assignments are used consistently. A represents MgATP^{2-} , B represents D-ribulose, K_a is the Michaelis constant for A, K_b is the Michaelis constant for B, and K_{ia} is the dissociation constant for the E-A complex. The Michaelis constants for ATP and D-ribulose are considerably lower than apparent K_m 's that have been reported earlier (7, 26).

Kinetic Studies with Substrate Analogs

The most direct kinetic approach to determining the substrate binding order in a sequential mechanism is the use of dead-end competitive inhibitors for each of the substrates (45). AMP was found to be a linear competitive inhibitor with respect to ATP and a linear noncompetitive inhibitor with respect to D-ribulose (Figs. 8 and 9). A number of compounds were examined as possible competitive inhibitors with respect to D-ribulose. Ribitol, xylitol, D-arabitol, L-arabitol, meso erythritol, L-ribulose, D-arabinose, D-ribose, and D-fructose show no inhibition of the reaction at 15 mM when the substrates are present at K_m levels. Dihydroxyacetone, however, gave inhibition that was competitive with respect to D-ribulose (Fig. 10).

These results are consistent with either a random substrate binding order or an ordered mechanism in which ATP adds first. Because both models predict similar rate equations, the one derived from Scheme I is given below:

$$\frac{1}{v} = \frac{1}{V} \left[1 + \frac{K_a}{A} \left(1 + \frac{I}{K_{ii}} \right) + \frac{K_b}{B} + \frac{K_{ia}K_b}{AB} \left(1 + \frac{I}{K_i} \right) \right] \quad (3)$$

Figure 8. Plot of the reciprocal of initial velocity (v) versus the reciprocal of the molar concentration of MgATP^{2-} at various, fixed concentrations of AMP^{2-}

The concentration of D-ribulose was held constant at $96.0 \mu\text{M}$. The MgATP^{2-} concentration was varied from $59.8 \mu\text{M}$ to 0.538 mM . AMP^{2-} was held at 7.87 mM (\circ), 5.89 mM (Δ), 3.93 mM ($+$), 1.96 mM (\times), and 0 mM (\diamond). Other experimental details are described under Experimental Procedure.

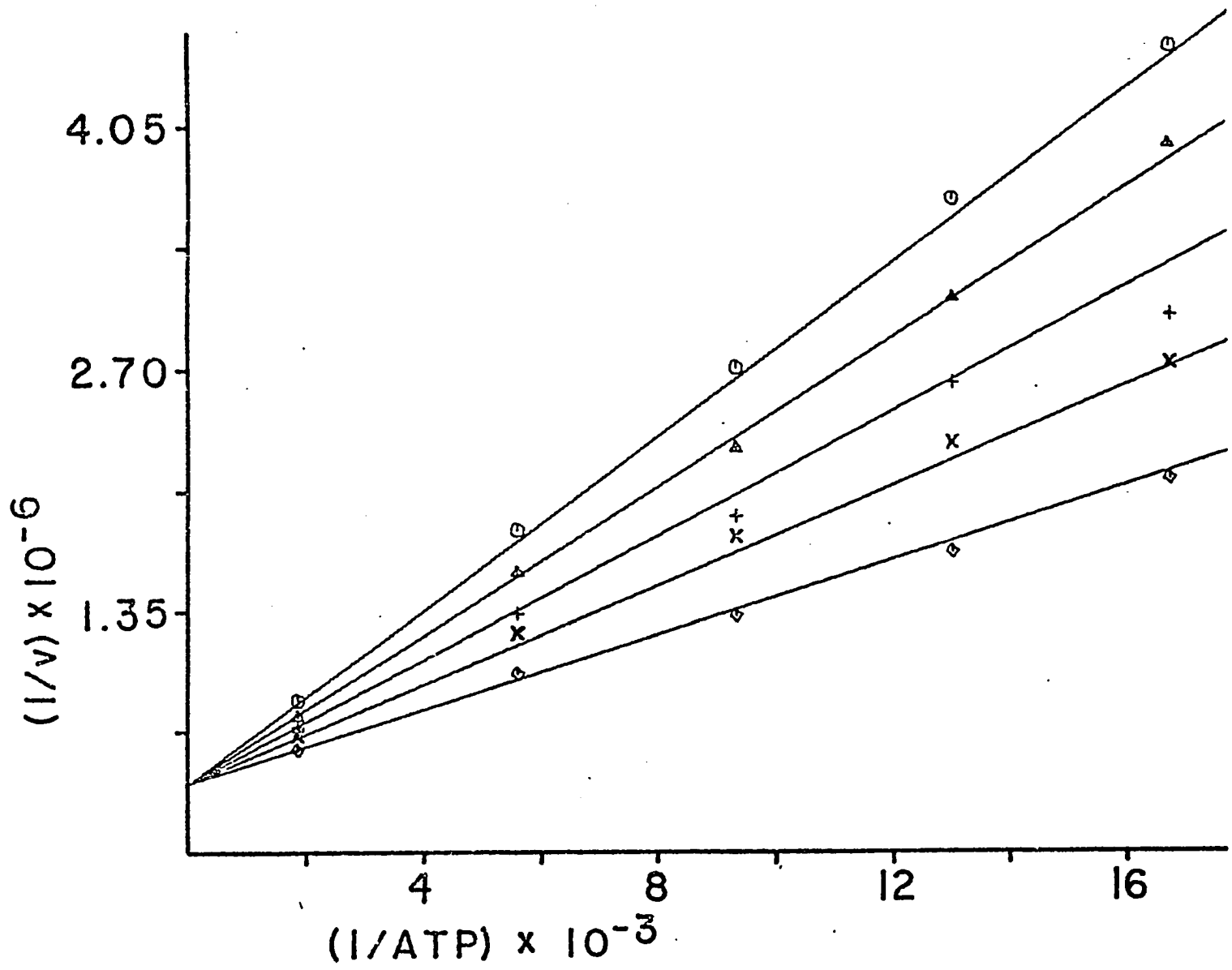


Figure 9. Plot of the reciprocal of initial velocity (v) versus the reciprocal of the molar concentration of D-ribulose at various fixed concentrations of AMP^{2-}

The concentration of MgATP^{2-} was held constant at $122 \mu\text{M}$. The concentration of D-ribulose varied from $53.3 \mu\text{M}$ to 0.48 mM . AMP^{2-} was held at 5.46 mM (\circ), 4.09 mM (Δ), 2.73 mM ($+$), 1.36 mM (\times), and 0 mM (\diamond). Other experimental details are described under Experimental Procedure.

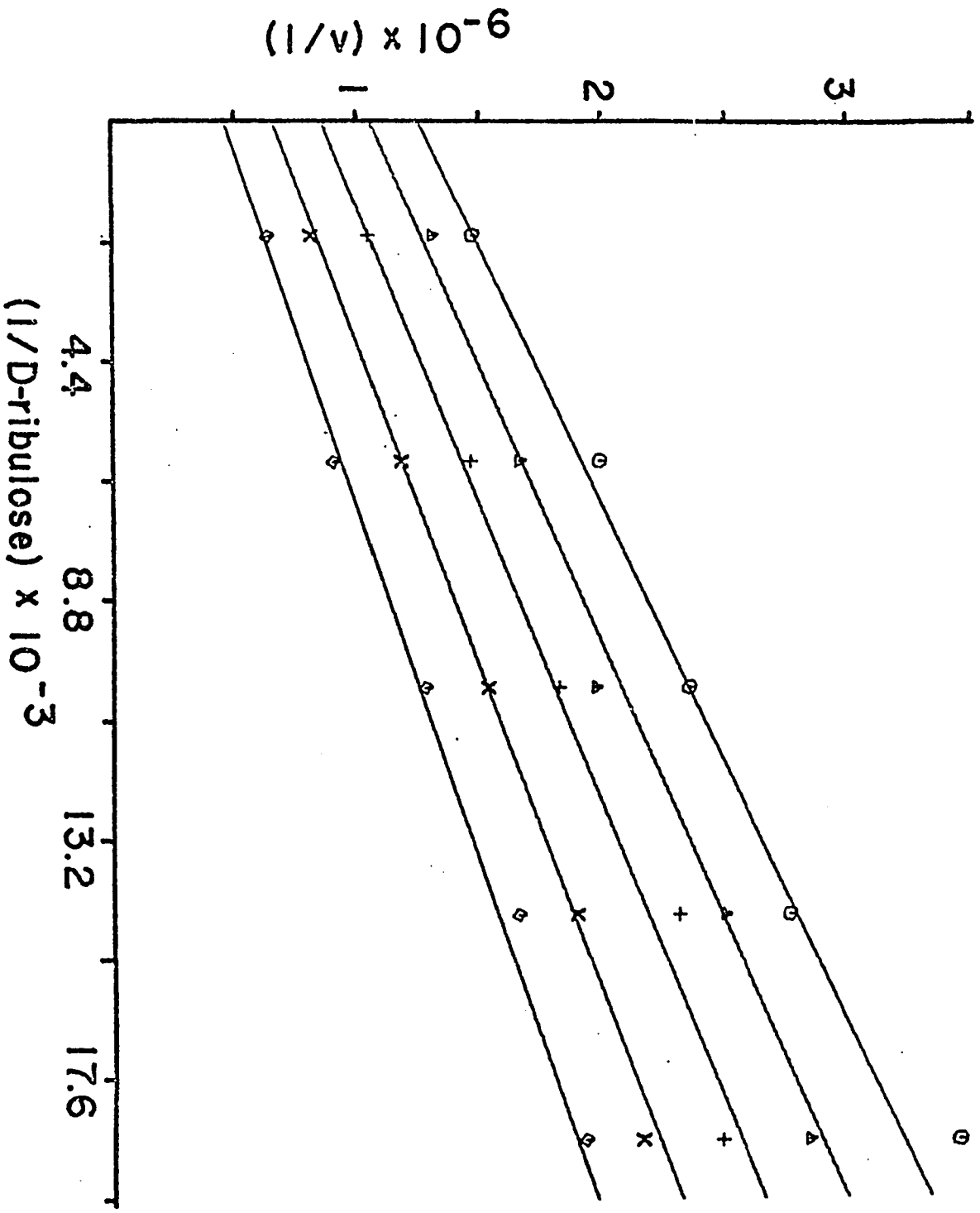
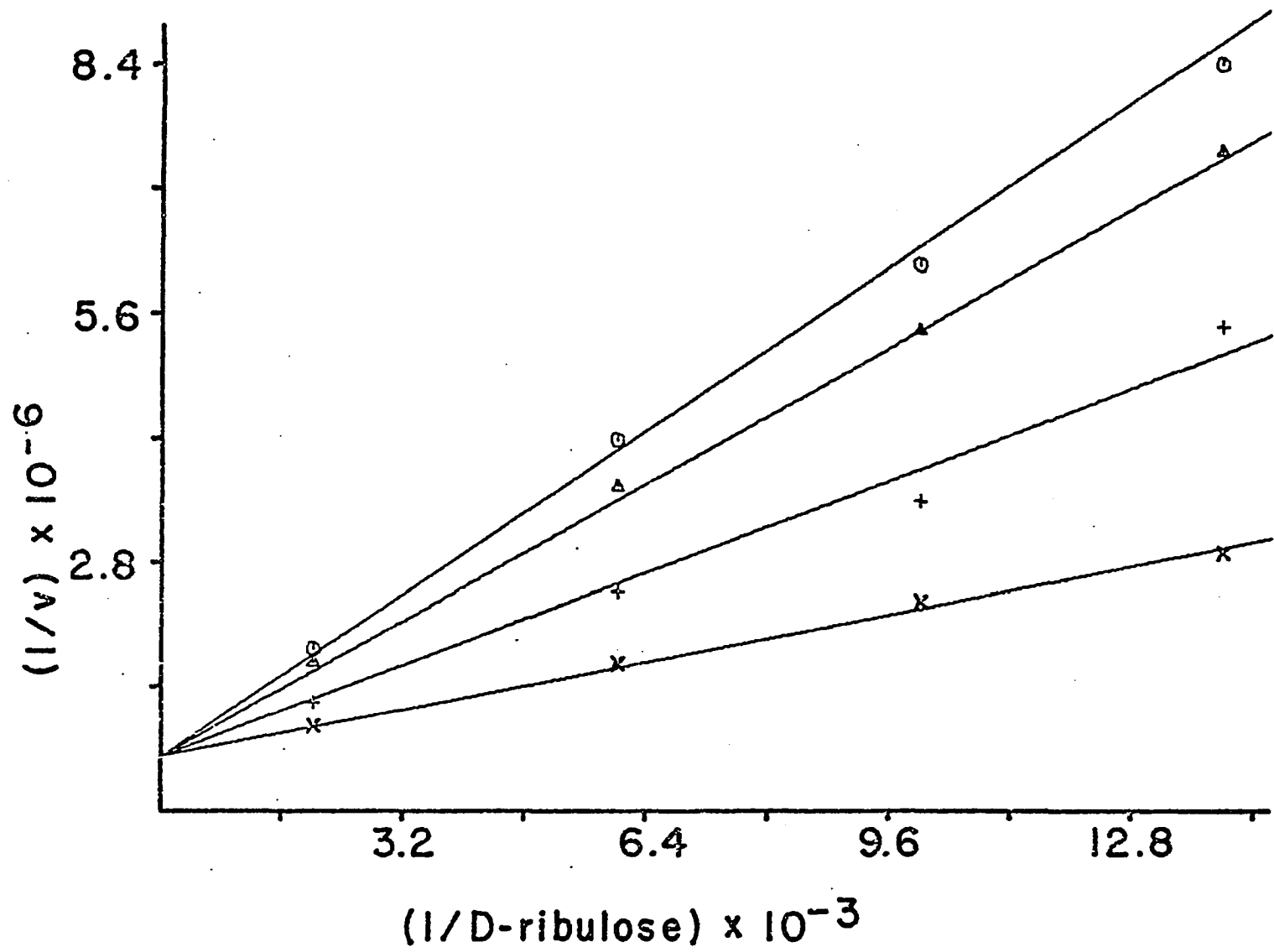
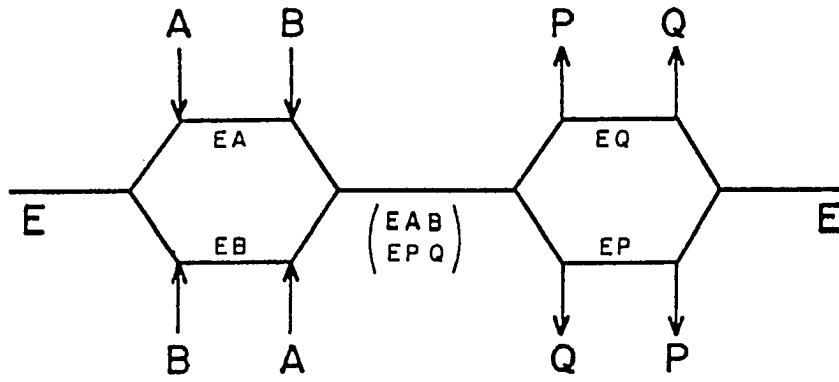


Figure 10. Plot of the reciprocal of initial velocity (v) versus the reciprocal of the molar concentration of D-ribulose at various fixed concentrations of dihydroxyacetone

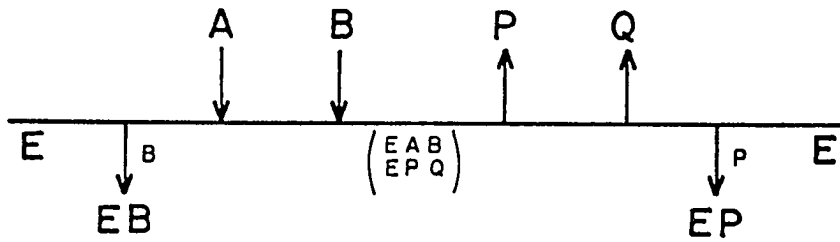
The MgATP^{2-} concentration was held constant at $81.1 \mu\text{M}$. The D-ribulose concentration varied from $71.5 \mu\text{M}$ to 0.501 mM . Dihydroxyacetone was held at 0.629 M (\circ), 0.484 M (Δ), 0.242 M ($+$), and 0 M (\times). Other experimental details are described under Experimental Procedure.



SCHEME I



SCHEME II



where $K_i = (E)(I)/(EI)$, $K_{ii} = (EB)(I)/(EBI)$, and I represents AMP.

To make a choice between the random and ordered mechanisms the competitive inhibitor for D-ribulose, dihydroxyacetone, is necessary. If the mechanism is rapid-equilibrium random, as shown in Scheme I, the following rate equation results;

$$\frac{1}{v} = \frac{1}{V_1} \left[1 + \frac{K_a}{A} + \frac{K_b}{B} \left(1 + \frac{I}{K_{ii}} \right) + \frac{K_{ia}K_b}{AB} \left(1 + \frac{I}{K_i} \right) \right] \quad (4)$$

where $K_i = (E)(I)/(EI)$, $K_{ii} = (EA)(I)/(EAI)$, and I represents dihydroxyacetone. If the mechanism is ordered with ATP adding first, the rate expression is given by equation (5).

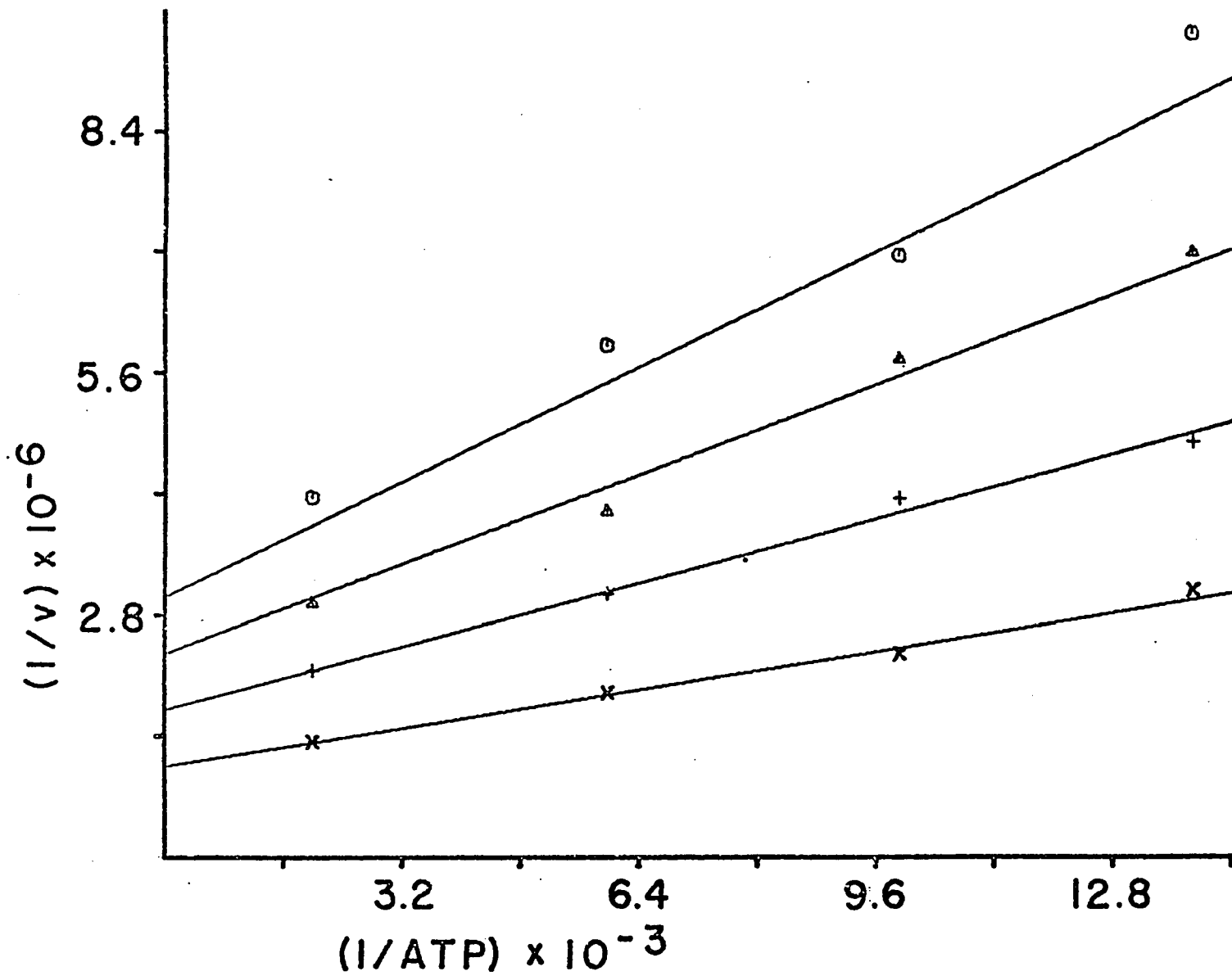
$$\frac{1}{v} = \frac{1}{V} \left[1 + \frac{K_a}{A} + \frac{K_b}{B} \left(1 + \frac{I}{K_i} \right) + \frac{K_{ia}K_b}{AB} \right] \quad (5)$$

Here, $K_i = (EA)(I)/(EAI)$ and, again, I represents dihydroxyacetone. Equation 5 predicts that the $\frac{1}{v}$ versus $\frac{1}{A}$ plot will show uncompetitive inhibition. That is not observed. When $1/v$ is plotted against $MgATP^{2-}$, at different fixed concentrations of dihydroxyacetone, the lines converge (Fig. 11). These data are consistent only with equation (4) and thus support the rapid-equilibrium random mechanism of Scheme I. The kinetic data of Figs. 6-11 were fitted to equations 2, 3 and 4 with the use of the computer. Values for the kinetic constants are reported in Table II.

As Frieden (46) has pointed out, the rapid-equilibrium ordered mechanism with two dead-end complexes shown in Scheme II is

Figure 11. Plot of the reciprocal of initial velocity (v) versus the reciprocal of the molar concentration of MgATP^{2-} at various, fixed concentrations of dihydroxyacetone

The D-ribulose concentration was held constant at 84.3 μM . The MgATP^{2-} concentration varied from 72.1 μM to 0.505 mM. Dihydroxyacetone was held at 0.639 M (\circ), 0.426 M (Δ), 0.213 M (\dagger), and 0 M (\times). Other experimental details are described under Experimental Procedures.



indistinguishable from the rapid-equilibrium random mechanism (Scheme I) on the basis of most kinetic criteria, including the use of substrate analogs (46,47). It was to eliminate this ambiguity that the isotope partitioning studies were undertaken.

Isotope Partitioning Studies

Isotope partitioning or pulse-chase techniques were first introduced into enzymology in 1962 (48) and have since been used by a number of workers (39,40,49,50). The protocol involved preincubating [^3H] D-ribulose with the enzyme, adding this mixture to a "chase" solution containing ATP and a large excess of unlabeled D-ribulose, incubating for 2 s, stopping the reaction, and then determining the radioactivity in the product, D-ribulose-5-P. The experiment (see Table III) eliminated Scheme II as an alternative because it excluded any rapid-equilibrium mechanism. If the mechanism is rapid equilibrium (i.e., the interconversion of the ternary complexes is rate limiting), then the [^3H] D-ribulose would not be trapped, but instead would equilibrate with unlabeled D-ribulose in the chase solution before turning over into product. In addition, the occurrence of significant trapping establishes the existence of a catalytically-active enzyme-ribulose complex.

Product Inhibition Kinetics

The product inhibition studies could not provide supporting evidence for Scheme I because D-ribulose-5-P did not inhibit the reaction (at concentrations up to 5 mM). ADP, however, proved to be a

Table III. Isotope partitioning with [³H]D-ribulose

The theoretical maximum trapping was calculated by using the dissociation constant for D-ribulose ($K_{ib} = 0.406$ mM) to determine the concentration of the E-D-ribulose complex at time zero. All bound substrate was assumed carried over into product. The control serves as a blank for radioactivity incorporated into product after the dilution of the label by the "chase" solution. Other experimental details are described under Experimental Procedure.

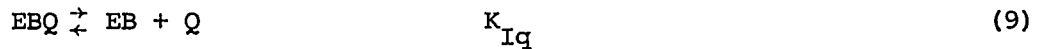
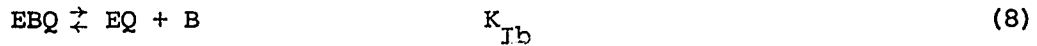
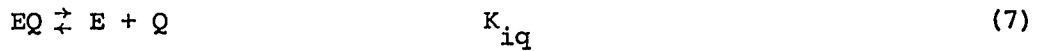
CPM found in D-ribulose 5-phosphate

Substrate	Control	Experimental	Net Trapping	Theoretical Maximum Trapping	% of Maximum Trapped
[³ H]D-ribulose	1,640	5,900	4,260	16,740	25
	1,640	4,780	3,140	16,740	19

linear competitive inhibitor with respect to ATP and a noncompetitive inhibitor with respect to D-ribulose (Figs. 12 and 13). These data, to be consistent with Scheme I, require that an abortive complex, E·ADP·D-ribulose, be present. The rate expression is:

$$\frac{1}{v} = \frac{1}{V_1} \left[1 + \frac{K_a}{A} \left(1 + \frac{Q}{K_{Iq}} \right) + \frac{K_b}{B} + \frac{K_{ia} K_b}{AB} \left(1 + \frac{Q}{K_{Iq}} \right) \right] \quad (6)$$

The interactions of Q (ADP) with the enzyme are:



These equilibria describe a closed cycle when one remembers that

EB = E + B, K_{ib} ; thus, these dissociation constants are not independent, being related by equation (10):

$$K_{iq} K_{Ib} = K_{Iq} K_{ib} \quad (10)$$

This allows calculation of all the constants in Eq. (10), and the results are tabulated in Table II.

Figure 12. Plot of the reciprocal of initial velocity (v) versus the reciprocal of the molar concentration of MgATP^{2-} at various, fixed concentrations of MgADP^{1-}

The D-ribulose concentration was held constant at $96.0 \mu\text{M}$. MgATP^{2-} was varied in the range $81.5 \mu\text{M}$ to $570 \mu\text{M}$. MgADP^{1-} was held at $261 \mu\text{M}$ (+), $174 \mu\text{M}$ (Δ), $87.0 \mu\text{M}$ (\square) and $0 \mu\text{M}$ (\circ). Other experimental details are described under Experimental Procedure.

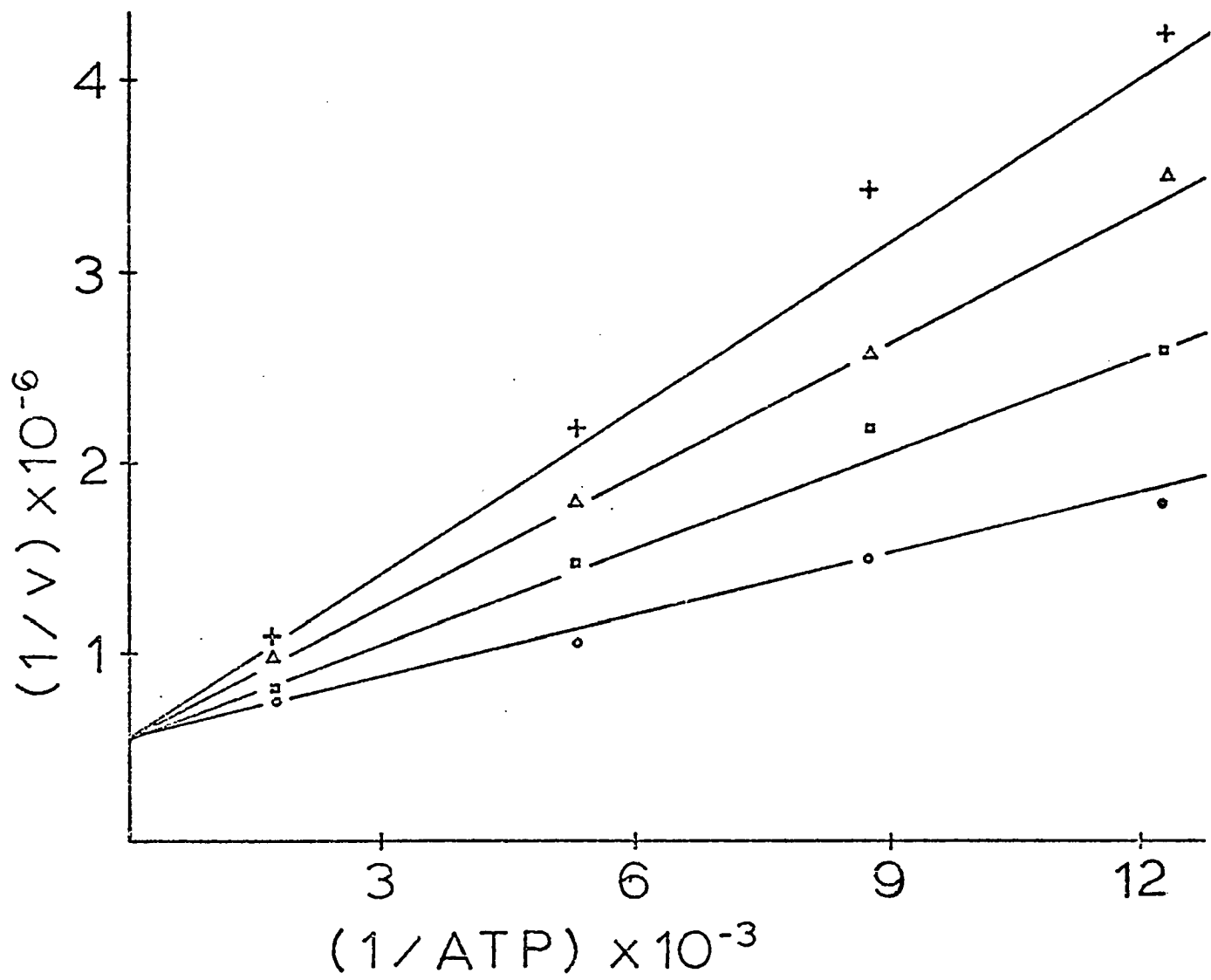
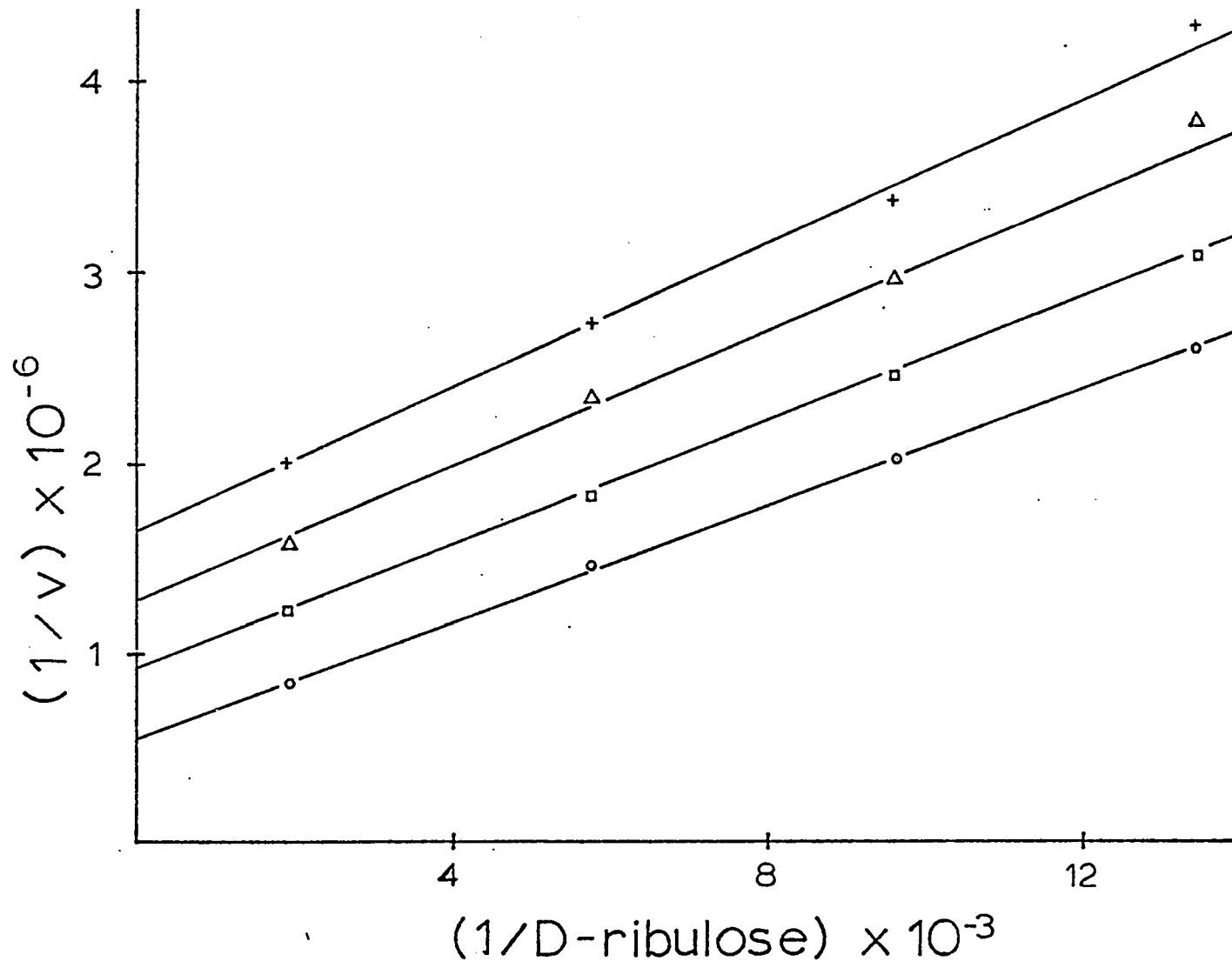


Figure 13. Plot of the reciprocal of initial velocity (v) versus the reciprocal of the molar concentration of D-ribulose at various, fixed concentrations of MgADP^{1-}

The MgATP^{2-} concentration was held constant at $86.6 \mu\text{M}$. D-ribulose was varied in the range $74.5 \mu\text{M}$ to $521 \mu\text{M}$. MgADP^{1-} was held at $125 \mu\text{M}$ (+), $83.2 \mu\text{M}$ (Δ), $41.6 \mu\text{M}$ (\square) and $0 \mu\text{M}$ (\circ). Other experimental details are described under Experimental Procedure.



DISCUSSION

Of the first two enzymes involved in ribitol metabolism in A. aerogenes, only ribitol dehydrogenase has been investigated to any extent. This has been true because of the lability of D-ribulokinase under the conditions of its purification and storage, which precludes any prolonged study. The purpose of this investigation, therefore, was to purify and stabilize D-ribulokinase to allow an investigation of its kinetic mechanism.

The purification was accomplished by eliminating the heat and alumina gel treatments from the purification protocol of Mortlock et al. (26) and by utilizing the techniques of high-resolution gel filtration and DEAE cellulose chromatography. Other purification techniques that proved unsatisfactory included hydroxylapatite chromatography, phosphocellulose chromatography, and the use of the general affinity matrix, Affi-Gel Blue.³ The final product was pure, by the criterion of SDS gel electrophoresis and gel filtration, with only two trace contaminants visible during gel electrophoresis. The enzyme ($M_r = 116,000$) is a dimer with a subunit molecular weight of 59,000.

The kinetic mechanism proved to be sequential, as shown by the initial-rate kinetics, and the problem of determining the order of substrate binding was approached by using AMP and dihydroxyacetone as

³Affi-Gel Blue, Bio-Rad, consists of cross-linked agarose coupled with the blue dye, Cibacron Blue F36A. It shows an affinity for many nucleotide-requiring enzymes.

substrate analogs. The inhibition patterns seen with these two compounds give support to a random Bi Bi mechanism (Scheme I). The product inhibition studied provided kinetic evidence for the formation of at least one abortive complex, E·D-ribulose·ADP. Isotope partitioning experiments that demonstrated trapping of [³H] D-ribulose gave additional support to the random model and ruled out the alternative mechanism shown in Scheme II. Indeed, no ordered scheme, in which D-ribulose does not react with the free enzyme to form a catalytically active complex, will show trapping of [³H] D-ribulose.

The evidence presented in this study lends support to the random Bi Bi model presented in Scheme I. Although the isotope partitioning studies indicate a steady-state mechanism for D-ribulokinase, the initial-velocity kinetics are consistent with a rapid-equilibrium model. This is particularly surprising inasmuch as the rate expression that has been derived for the two-substrate, steady-state random mechanism (51) predicts nonlinear reciprocal plots with either substrate. The same phenomenon has also been observed with yeast hexokinase for which the kinetic evidence suggests a rapid-equilibrium random model; but, the equilibrium isotope-exchange studies demonstrate an ATP ↔ ADP exchange that is approximately twice the glucose ↔ glucose-6-phosphate exchange. In an attempt to rationalize these findings, Rudolph and Fromm (51) used the digital computer to simulate the steady-state random mechanism by utilizing various combinations of rate constants. Their findings are consistent with the experimental observations and indicate that the rapid-equilibrium assumption can be a good approximation to a

steady-state model. Danenburg and Cleland also came to similar conclusions for yeast hexokinase (52).

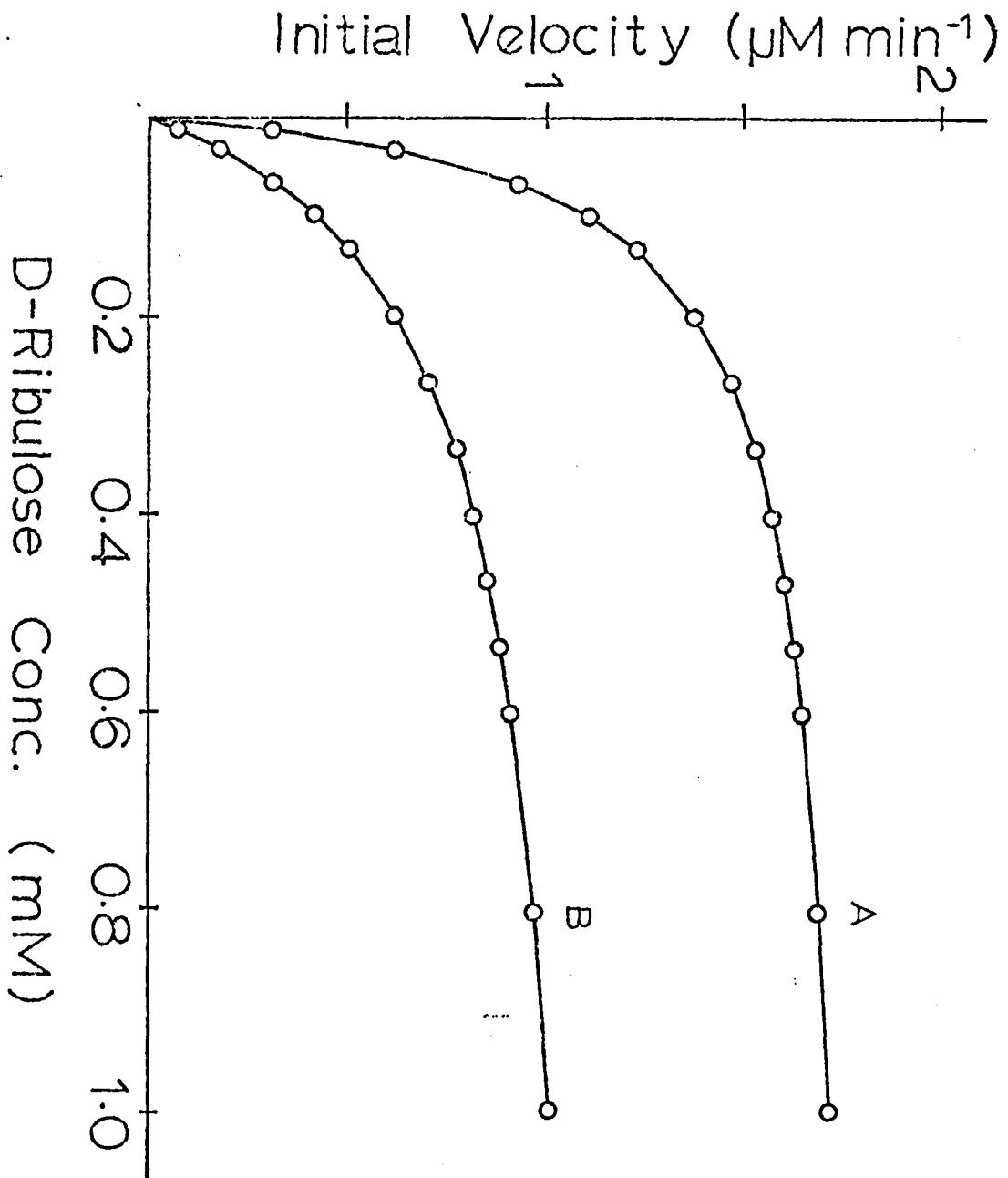
One point not resolved in these studies is the effect of D-ribulose-5-P on the reaction velocity. This product caused no inhibition at concentrations up to 5 mM; however, at higher levels, an apparent activation was observed. The effect was seen in both the [^{14}C] ATP stopped-time assay and the spectrophotometric coupled assay for ADP. Because the activation in the absence of D-ribulose-5-P can be mimicked by simply raising the ionic strength of the assays, the effect observed probably is not due to ribulose-5-P per se, and further investigation will be required before definitive conclusions may be drawn.

Table II indicates that D-ribulokinase has a greater affinity for MgADP^{1-} ($K_{\text{Iq}} = 20 \mu\text{M}$) than it does for MgATP^{2-} ($K_{\text{a}} = 54 \mu\text{M}$). Because the intracellular concentrations of ATP and ADP in E. coli, a closely related organism, have been determined to be 2 and 0.7 mM, respectively (53), D-ribulokinase will be saturated with these nucleotides in vivo.

The plot shown in Fig. 14 was calculated from Eq. 6 and the kinetic constants listed in Table II, assuming the MgATP^{2-} and MgADP^{1-} concentrations were 2 mM and 0.7 mM, respectively. The maximum velocity is reached when the D-ribulose concentration is about 1 mM, however that maximum velocity is less than half of V_1 . This simplistic approach does not take into account that the levels of free MgADP^{1-} and MgATP^{2-} will be considerably lower than the total nucleotide concentrations reported by Lowry et al. (53). There is little effect on the plot in Fig. 14 of lowering the MgATP^{2-} and MgADP^{1-} concentrations, while

Figure 14. A theoretical plot of initial velocity (v) versus the molar concentration of D-ribulose

The two curves were calculated from equation (6) and the kinetic constants listed in Table II. A. The MgATP^{2-} and MgADP^{1-} concentrations were 2 mM and 0.7 mM, respectively. B. The MgATP^{2-} and MgADP^{1-} concentrations were 50 μM and 17.5 μM , respectively.



maintaining them in the same ratio. The greatest changes are observed when the nucleotide concentrations approach K_m levels (Fig. 14). Such low concentrations are not observed in living cells.

LITERATURE CITED

1. Wood, W. A., and Tai, J. V. (1958) Bacteriol. Proc. p. 99.
2. Fromm, H. J. (1958) J. Biol. Chem. 233, 1049-1052.
3. Nordlie, R. C., and Fromm, H. J. (1959) J. Biol. Chem. 234, 2523-2531.
4. Wood, W. A., McDonough, M. J., and Jacobs, L. B. (1961) J. Biol. Chem. 236, 2190-2195.
5. Fromm, H. J., and Bietz, J. A. (1966) Arch. Biochem. Biophys. 115, 510-514.
6. Fromm, H. J., and Nelson, D. R. (1962) J. Biol. Chem. 237, 215-220.
7. Fromm, H. J. (1959) J. Biol. Chem. 234, 3097-3101.
8. Bisson, T. M., Oliver, E. J., and Mortlock, R. P. (1968) J. Bacteriol. 95, 932-936.
9. Bisson, T. M., and Mortlock, R. P. (1968) J. Bacteriol. 95, 925-931.
10. LeBlanc, D. J., and Mortlock, R. P. (1972) Arch. Biochem. Biophys. 150, 774-781.
11. Mortlock, R. P., and Wood, W. A. (1964) J. Bacteriol. 88, 838-844.
12. Mortlock, R. P. (1976) Adv. Microb. Physiol. 13, 1-53.
13. Neish, A. C., and Simpson, F. J. (1954) Can. J. Biochem. Physiol. 32, 147-153.
14. Altermatt, H. A., Simpson, F. J., and Neish, A. C. (1955) Can. J. Biochem. Physiol. 33, 615-621.
15. Simpson, F. J., Wolin, M. J. and Wood, W. A. (1953) J. Biol. Chem. 230, 457-472.
16. Anderson, R. L., and Wood, W. A. (1962) J. Biol. Chem. 237, 296-303.
17. Lin, E. C. C. (1961) J. Biol. Chem. 236, 31-36.
18. Fossitt, D., Mortlock, R. P., Anderson, R. L., and Wood, W. A. (1964) J. Biol. Chem. 239, 2110-2115.

19. Rigby, P. W. J., Burleigh, B. D., and Hartley, B. S. (1974) Nature 251, 200-204.
20. Charnetzky, W. T., and Mortlock, R. P. (1970) Bacteriol. Proc. 137.
21. Inderlied, C. B., and Mortlock, R. P. (1977) J. Mol. Evol. 9, 181-190.
22. Lin, E. C. C., Hacking, A. J., and Aguilar, J. (1976) BioScience 26, 548-555.
23. Wu, T. T., Lin, E. C. C., and Tanaka, S. (1968) J. Bacteriol. 96, 447-456.
24. Lerner, S. A., Wu, T. T., and Lin, E. C. C. (1964) Science 146, 1313-1315.
25. Scangos, G. A., and Reiner, A. M. (1978) J. Bacteriol. 134, 501-505.
26. Mortlock, R. P., Fossitt, D. D., Petering, D. H., and Wood, W. A. (1965) J. Bacteriol. 89, 129-135.
27. Stayton, M. M., and Fromm, H. J. (1979) J. Biol. Chem. 254, 3765-3771.
28. Glatthaar, C., and Reichstein, T. (1935) Helv. Chim. Acta 18, 80-81.
29. Reichstein, T. (1934) Helv. Chim. Acta 17, 996-1002.
30. Mortlock, R. P., and Wood, W. A. (1965) Bacteriol. Proc. p. 82.
31. Lieberman, I. (1956) J. Biol. Chem. 223, 327-339.
32. Rudolph, F. B., Purich, D. L., and Fromm, H. J. (1968) J. Biol. Chem. 243, 5539-5545.
33. Davis, B. J. (1964) Ann. N.Y. Acad. Sci. 121, 404.
34. Weber, K. and Osborn, M. (1969) J. Biol. Chem. 244, 4406-4412.
35. Andrews, P. (1964) Biochem. J. 91, 222-223.
36. Rudolph, F. B. and Fromm, H. J. (1969) J. Biol. Chem. 244, 3832-3839.
37. Morrison, J. F. (1968) Anal. Biochem. 24, 106-111.
38. Newton, H. F., Ott, D. B., and Kerr, B. N. (1956) Nucleonics 14, 42-45.

39. Raushel, F. M., and Cleland, W. W. (1977) Biochemistry 16, 2176-2181.
40. Rose, I. A., O'Connell, L., Litwin, S., and Bar, Tana, J. (1974) J. Biol. Chem. 249, 5163-5168.
41. Bray, G. A. (1960) Anal. Biochem 1, 279-285.
42. Siano, D. B., Zyskind, J. W., and Fromm, H. J. (1975) Arch. Biochem. Biophys. 170, 587-600.
43. Cleland, W. W. (1963) Biochim. Biophys. Acta 67, 104-137.
44. Alberty, R. A. (1953) J. Am. Chem. Soc. 75, 1928-1932.
45. Fromm, H. J., and Zewe, V. (1962) J. Biol. Chem. 237, 3027-3032.
46. Frieden, C. (1976) Biochem. Biophys. Res. Commun. 68, 914-917.
47. Fromm, H. J. (1976) Biochem. Biophys. Res. Commun. 72, 55-60.
48. Krishnaswamy, P. R., Pamibjans, V., and Meister, A. (1953) J. Biol. Chem. 237, 2932-2940.
49. Rochovansky, O., and Ratner, S. (1967) J. Biol. Chem. 242, 2839-3849.
50. Uyeda, K. (1970) J. Biol. Chem. 245, 2268-2180.
51. Rudolph, F. B., and Fromm, H. J. (1971) J. Biol. Chem. 246, 6611-6619.
52. Danenburg, K., and Cleland, W. W. (1975) Biochemistry 14, 28-39.
53. Lowry, O. H., Carter, J., Ward, J. B., and Glaser, L. (1971) J. Biol. Chem. 246, 6511-6521.

APPENDIX

The following is a list of work completed and published by the candidate. An abstract of each paper is included.

Stayton, Mark M. and Herbert J. Fromm (1978) A Computer Analysis of the Validity of the Integrated Michaelis-Menten Equation. J. Theor. Biol. 78, 309-323.

The validity of assumptions made in integrating the Michaelis-Menten equation (i.e. the steady-state assumption) was examined by simulating the model on the digital computer. Time courses thus obtained by numerical integration were compared with data generated by the three most common forms of the integrated equation. Agreement was good within specified limits, the chief exception being the early transient phase of the reaction. The observed differences were very much less than theoretical estimates of the maximum error, even when rate constants were chosen that should exaggerate that error.

Stayton, Mark M. and Herbert J. Fromm (1979) Guanosine 5'-diphosphate-3'-diphosphate Inhibition of Adenylosuccinate Synthetase. J. Biol. Chem. 254, 2579-2581.

The mechanism of ppGpp inhibition of adenylosuccinate synthetase (EC 6.3.4.4) was examined. Initial rate kinetic studies demonstrate that ppGpp inhibition is competitive with respect to GTP and noncompetitive with respect of L-aspartate and IMP. This is in contrast to an earlier report (Gallant, J., Irr, J., and Cashel, M. (1971) J. Biol. Chem. 246, 5812-5816), which suggested that ppGpp did not bind at the GTP site. Possible reasons for the discrepancy are discussed. The potency of the ppGpp inhibition is confirmed.

Stayton, Mark M. and Herbert J. Fromm (1979) Purification, Properties and Kinetics of D-Ribulokinase from Aerobacter aerogenes. J. Biol. Chem. 254, 3765-3771.

The enzyme D-ribulokinase from Aerobacter aerogenes was purified to near homogeneity. The molecular weight, as determined by Sephacryl gel chromatography, is 116,000. The subunit molecular weight, determined by sodium dodecyl sulfate-gel electrophoresis, is 59,000, suggesting that D-ribulokinase is a dimer of identical subunits. Initial rate kinetic studies, involving substrate analogs and products, were carried out. These investigations support a kinetic mechanism of the Random Bi Bi type. Isotope partitioning, utilizing D-[³H]Ribulose, indicates that the mechanism is steady state Random Bi Bi.

The following is a summary of work carried out during the past year.

Stayton, Mark M. and Herbert J. Fromm (1980) Positional Isotope Exchange Studies on Adenylosuccinate Synthetase from Escherichia coli, Manuscript in preparation.

Adenylosuccinate synthetase from Escherichia coli was purified to near homogeneity. The techniques utilized include anion exchange chromatography, group-affinity chromatography and hydrophobic chromatography. Its native molecular weight is 100,000 (determined using molecular exclusion gel chromatography) and its molecular weight (determined under denaturing conditions by SDS gel electrophoresis) is 48,000. This data suggests that adenylosuccinate synthetase is a dimer of identical subunits. Positional isotope exchange experiments were carried out as a probe of the chemical mechanism. Partial reaction mixtures (containing chemically synthesized [γ -¹⁸O₄]GTP, enzyme, MgCl₂ and one of the remaining two substrates) catalyzed the intramolecular exchange of the β - γ bridgehead oxygen atom for a β -nonbridgehead oxygen atom. This exchange was also observed in the absence of either of the other two substrates. The results, based on low-field ³¹P NMR spectra are preliminary, but suggest that the enzyme catalyzes the transient hydrolysis of GTP in the active

site. An attempt to identify a phosphoryl enzyme intermediate was unsuccessful. An L-aspartate-activated [^{14}C] GDP \rightleftharpoons GTP exchange reaction was discovered.

ACKNOWLEDGMENTS

I would particularly like to express my gratitude to Dr. Herbert Fromm for the perceptive guidance he has provided during the past five years.

I also thank my family, Tary, Sean, and Sarah, whose love, companionship and good humor have greatly enriched my life. I appreciate their support.

I acknowledge the help I have received from the many friends with whom I have worked. Their companionship has made this educational experience very enjoyable.